Journal of Fundamental and Applied Sciences

Research Article

ISSN 1112-9867

Available online at http://www.jfas.info

SYNTHESIS, CHARACTERIZATION, CORROSION INHIBITION OF MILD STEEL BY TWO SCHIFF BASES IN HCL AND DENSITY FUNCTIONAL THEORY STUDIES

A. Madani[*1, 2], L. Sibous[1], E. Bentouhami[2]

[1]Laboratoire d'Électrochimie et Matériaux, Département de Génie des Procédés, Faculté de Technologie, Université Ferhat Abbas, Sétif-1, 19000- Algeria

[2]Laboratoire de Chimie, Ingénierie Moléculaire et Nanostructures, Université deSétif1, 19000- Algeria

Received: 06 December 2019 / Accepted: 28 February 2021 / Published online: 01 May 2021

ABSTRACT

In this study, two Schiff bases namely (E,E)-N,N'-biphenyl-4-4'diylbis[1-(furan-2-yl)methanimine] (BEFu) and3-[(Z)-N(4'-aminobiphenyl-4yl)ethanimidoyl]-2-hydroy-6-methyl-4H-pyran-4-one (BEDh) have been synthesized and characterized using UV-visible, FTIR, and NMR techniques. The corrosion inhibition study of BEFu and BEDh was investigated for mild steel corrosion in 1M hydrochloric acid medium using weight loss method, potentiodynamic polarization, EIS techniques, and Density Functional Theory (DFT). The results showed that the inhibition efficiency increasing with concentration and revealing a mixed-type inhibitor of predominantly anodic type. To explain the inhibition abilities of those molecules adsorbed on the mild steel surface, quantum chemical calculations have been performed using DFT. The HOMO and LUMO energies were calculated to determine the global reactivity indexes. The experimental and theoretical results were in good agreement.

Key words: weight loss method; inhibitor; polarization curves; DFT; HOMO; LUMO.

Author Correspondence, e-mail: abdelghanima@yahoo.fr

doi: http://dx.doi.org/10.43 14/jfas.v13i2.13

1. INTRODUCTION

The compounds containing carbonyls units such aldehydes and ketones are used as chief products in many organic synthesis, due to the high reactivity of the C=O, the difference of the carbon and oxygen electronegative atoms [1]. Schiff basis are compounds of general formula $R_1R_2C=NR_3$ in which the roots R_1, R_2 and R_3 may be alkyls, cycloalkyles or aromatics nucleic groups. They have been first synthesized by the German chemist *Hugo Schiff* in 1864 [2], for such they are called thus, i.e. "Schiff bases". Atoms suppliers of electron pairs such N, O, S that ligand Schiff bases' contains witnesses their use in several applications [3]. A large number of different Schiff base derivatives are used in materials science such solar shell [4], optical switching [5], third order non-linear optics (NLO) [6], electrochemical sensing [7], Langmuir films and photo-initiated polymerization [8]. They are famous for their biological application as antibacterial [9].Schiff base compounds containing heteroatoms with electronic lone pair (N, O and S), or π systems, or conjugated bonds, or aromatic rings, are generally considered to be effective corrosion inhibitors, as important heterocyclic compounds [10-18]. Schiff's bases are also used as efficient inhibitors for mild steel corrosion in HCl media due to the presence of –C=N– group [19,20]. The lone pair of electrons on N, O and S atoms, and the planarity of the molecule are useful for its adsorption to the metal surface [21,22]. This work represents synthesis of two new Schiff bases, (BEDh) and (BEFu). These compounds have characterized by various spectroscopic means as the Infra-red, UV-visible, ^{1}H- NMR and ^{13}C-NMR. The corrosion inhibition properties of the investigated Schiff bases were evaluated for mild steel corrosion in 1M of HCl using weight loss, polarization curves and electrochemical impedance. The optimized geometry of their molecular properties such equilibrium energy, frontier orbital energy gap, molecular electrostatic potential energy gap, dipole moment, polarizabilityand the electronic structures have been optimized and tested at Density Functional Theory, (DFT), level employing the basis set 6-31G(*d*,*p*).

2. EXPERIMENTAL DETAILS

2.1 Materials

The used chemicals and solvents were analytical reagent grade used without further purification. 4,4'-diaminobiphenyl(benzidine), 2-carboxaldehyde furan, Déhydroacitic acid and HCl (hydrochloric acid, 37%) purchased from Aldrich. The test solution of 1M of HCl was prepared from analytical grade reagent (37% HCl) and double-distilled water. The measurements were carried out in 1M of HCl in the absence and presence of inhibitors, the concentrations varied from 1.0×10^{-6} M to 1.0×10^{-3}M in 1 M HCl. The mild steel specimens

having the dimension (0.2×0.25×0.50cm) and the working electrode (working surface 0.5cm^2) was selected from a mild steel rod with a chemical composition (in wt%) as follows: 0.09%C, 0.014%P, 0.058%Si, 0.91%Mn, 0.002%S, 0.043% V, 0.044% Al, 0.057% Nb and 98,782%Fe, were used for gravimetric and potentiodynamic polarization studies.

2.2. Synthesis of Schiff base compounds

2.2.1 Synthesis of BEFu

The condensation reaction in a 2:1 molar ratio of 2-carbaxaldehyde furan (1.0ml, 5.4mmol) and the 4,4'-diaminobiphenyl (0.5 g, 2.7mmol) in absolute ethanol was refluxed for 4 h at 55°C (Scheme 1), from which yellow solution then kept at room temperature. The yellow precipitate was filtered, washed with ethanol and dried in vacuum. FT-IR (cm^{-1}), 3025-3112 (aromatic C–H), 1591–1610 (C=N), 1360–1470 (phenyl rings C=C, C–C). UV-Vis (DMF, λ_{max}=238 and 366nm).^{1}H-NMR (DMSO-d$_6$, δ (ppm), 400MHz): 6.73 (t, 2H, H2, H'2); 7.18 (d, 2H, H3, H'3); 7.36 (d, 4H, H6, H'6,H8, H'8); 7.75 (d, 4H, H5, H'5,H7, H'7); 7.96 (d, 2H, H1 ,H'1); 8.52, (s, 2H, H4, H'4). ^{13}C NMR (DMSO-d$_6$), δ (ppm), 400MHz): 114.05(C21, C26); 117.57 (C22,C24); 122.15- 121.99 (C2,C6,C10,C11,); 127.72-126.44 (C1, C5,C8, C9); 137.77 (C7, C3); 146.96 (C4, C12); 148.59(C20, C25); 150.66(C15, C16); 152.48 (C18, C17).Solubility, Soluble in MeOH, DMSO and DMF, Yield, (63%). *Mp*: 181-183°C. $C_{22}H_{16}N_2O_2$. Mol. Wt. 340.37 g/mol).

2.2.2 Synthesis of BEDh

The BD Schiff base was synthesized by reaction in a 1:1 molar ratio of déhydroacitic acid (0.3g, 1.6mmol) and the 4,4'-diaminobiphenyl (3.0g, 1.6mmol) in absolute ethanol for 4h at 55 °C (Scheme 1). The crystalline product was obtained by slow evaporation at room temperature. The crystalline product that formed was filtered and washed with cold ethanol and dried over anhydrous silica gel. *3*-[(1Z)-N(4'-aminobiphenyl-4yl)ethanimidoyl]-2-hydroy-6-methyl-4H-pyran-4 one: FT IR, υ= 1595 cm^{-1} (C=N);υ=1665 cm^{-1} (C=O); υ=1043cm-^{1} (C-O-C); υ= 1356 cm^{-1} (OH). UV-Vis (DMF, λ_{max}=271 and 299 nm), Solubility: Soluble in MeOH, EtOH and DMSO, Yield (62%). *Mp*: 250 252°C. $C_{20}H_{18}N_2O_3$. Mol.Wt=334.35g/mol.

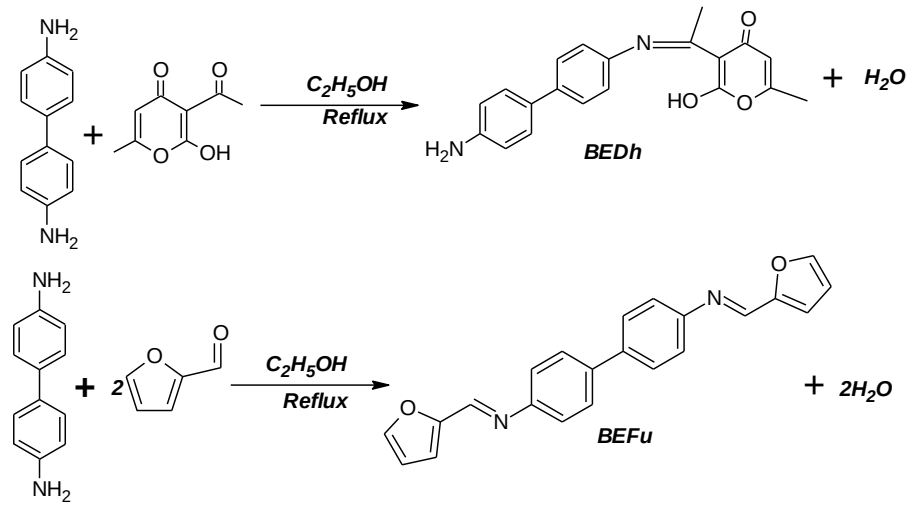

Scheme.1. Synthesis of Schiff base compounds **BEDh** and **BEFu**

2.3 Characterization

The infrared spectra were recorded with a SHIMADZU FTIR 8400Sseries FT-IR spectrophotometer using KBr disks. The UV-visible spectra were obtained in DMF with a SHIMADZU UV-1700 spectrophotometer. The ^{1}HNMR spectra were recorded on Brukre AC 400-MHZ advance spectrophotometer in DMSO-d_6 as the solvent and tetramethylsilane (TMS) as an internal standard at room temperature. , the chemical shifts are given in ppm scale and coupling constants J(values) are expressed in Hertz, multiplicity is indicated as **s**(singlet),**d**(doublet), **t**(triplet)and **m**(multiplet). The melting points were determined with fusiometer without correction.

2.4. Inhibitor's study

2.4.1. Weight loss Measurement

Gravimetric experiments were performed according to the standard methods [23]. The specimens, with dimension of 3.0x2.6x1.0cm, were polished with emery paper, and then washed with distilled water and acetone. The initial weight of mild steel was measured using an analytical balance. Then, the prepared specimens were immersed in 100 mL of 1M HCl with and without various concentrations of Schiff bases BEDh or BEFu at 25°C in aerated condition. After 24h of immersion, the specimens were taken out, rinsed thoroughly with distilled water, dried and weighed accurately again.

The weight loss Δw (mg) was used to calculate the corrosion rate W(mg.cm^{-2}.h^{-1}). The corrosion rate was calculated bay using the following equation [24].

$$W = \frac{\Delta w}{S \times t} = \frac{w2 - w1}{S \times t} \qquad (1)$$

Where Δw is the average weight loss (mg), w_1 and w_2 are the mass of the test specimen before and after corrosion, S is the surface area (cm^2) and t is the immersion time (h). The inhibition efficiency (*IE (%)*) and surface coverage (θ) of the XC48 by the molecules of the inhibitor were determined by the following equations [25, 26].

$$IE(\%) = \frac{W_0 - W}{W_0} \times 100 \qquad (2)$$

$$\theta = \frac{W_0 - W}{W_0} \qquad (3)$$

Where W and W_0 are the corrosion rates in the absence and presence of the inhibitors

2.4.2. Potentiodynamic polarization measurement (Tafel)

The electrochemical measurements were performed using PGZ 301 Voltalab 40 and Voltamaster 4 software for the calculation of charge density. The mild steel was used as the working electrode, a platinum electrode was used as the counter electrode and the reference electrode was a saturated calomel electrode (SCE). The surface are exposed to the electrolyte is 0.5 cm^2 and the working electrode was immersed in the test solution for 30 minutes to a establish steady-state in the open circuit potential (OCP) corresponding to the corrosion potential (E_{corr}) of the working electrode. After measuring the open circuit potential, potentiodynamic polarization curves were obtained with a 0.5 mV/s scan rate in the -800 to -250 mV potential range. The corrosion inhibition efficiency was calculated from the corrosion current values determined from the Tafel extrapolation method using the experimental relation. The inhibition efficiency *Wp(%)* obtained from polarization measurement was calculated according following equation.

$$Wp(\%) = \left(\frac{i_{corr} - i_{corr(inh)}}{i_{corr}}\right) x\ 100 \qquad (4)$$

Where i_{corr} and $i_{corr(inh)}$ are the corrosion current densities in the absence and presence of the inhibitor, respectively.

2.4.3 .Impedance spectroscopy (EIS) measurement

The electrochemical impedance spectroscopy (EIS) measurement was carried out at the frequency range of 100 kHz10mHz at the steady open circuit potential (OCP) with an amplitude of 10 mV. The charge transfer resistance (Rct) and double layer capacitance (Cdl) were calculated from Nyquist plots as described elsewhere [27, 28]. The inhibition efficiency and the interfacial double layer capacitance were calculated by equations (5) and (6):

$$WE(\%) = \frac{R_{ct} - R_{ct_0}}{R_{ct}} \qquad (5)$$

$$C_{dl} = \frac{1}{2\pi Fmax} x \frac{1}{R_{ct}} \qquad (6)$$

Where F_{max} is the maximum frequency, R_{ct} and R_{ct0} are the charge transfer resistances in the absence and presence of inhibitors, respectively.

2.5 Theoretical studies

All calculations were carried out using Density Functional Theory (DFT). The DFT-B3LYP method, with the basis set 6- 31G (d,p). Geometry optimization, an important issue in molecular mechanics, was performed as the first task of the computational work for the synthesized molecules. It requires in particular the sensitivity of the interaction energy with respect to the change of the molecule's shape which is in general induced by the movement of the nuclei positions. The molecular structure, vibrational frequencies and energies of the optimized geometries of BEDh and BEFu were calculated employing the DFT [29] method using Gaussian 09 [30] program package employing 6-31G(d,p) basis set based on Becke's three parameters (local, non-local, Hartree-Fock) hybrid exchange functional with Lee-Yang-Parr correlation functional (B3LYP) [31,32]. The basis set 6-31G(d,p) augmented by 'd' polarization functions on heavy atoms and 'p' polarization functions on hydrogen atoms as well as diffuse functions for both hydrogen and heavy atoms were used [33,34].

3. RESULTS AND DISCUSSIONS

3.1. Chemistry

The compounds structures thus obtained were identified and characterized through UV-visible, FTIR, and ^{1}H-NMR and ^{13}C-NMR spectroscopy. Both compounds (BEDh and BEFu) proved to be readily soluble in polar solvents. In the light of the spectroscopic results, it is to be asserted that the products stability is quite consistent. Furthermore, the DFT theoretical calculations witnessed harmonic relative accordance with our synthesized products molecular structures. Besides, FTIR Tests indeed confirmed the presence of Schiff bases in the synthesized products that manifest saturation carbon (sp^3) absorption bands at 2930~2290 cm^{-1}. Likewise, strong intensity band concluded from the IR spectra Schiff base ligands at 1577-1614cm^{-1} is normally due to the "υC=N". In the whole, the FTIR absorptions and intensities shown witness that the condensation of the carbonyl compound with the "NH_2" group of 4, 4'-diaminobiphenyl have indeed taken place. As for the evident band of 1540 cm^{-1}, it results of the "NH" deformation vibration and the medium bands located at the 1580-1600 cm^{-1}spectrum zone, they manifest

owing to the stretching of various aromatic cycles "C=C" vibrations of the synthesized ligands. In the other hand, the Schiff base ligands ^{1}H NMR spectra, the full integral intensities of every signal comply clearly with the number of different types of protons displayed in the spectrum. In addition, the 8.52ppm singlet signal related to the "CH=N" proton (1H) proves formation of the Schiff base after condensation of the carbonyl compound with the 4,4'-diaminobiphenyl. The proved fact shows as well the disappearance of peaks around 9.98 δ that correspond to the aldehydic proton. In the same spectrum, the 6, 73 – 7, 96 ppm noticed singlet and doublet are assigned to the heterocyclic protons.

3.2. Corrosion inhibition tests

3.2.1. Weight loss measurement

The Gravimetric data after 24 h were assessed and listed in Table 1. Following the given data, the maximum inhibition efficiency $(IE_g(\%)$ increase to about 98.62% and 95.73% for 2.5×10^{-4}M concentration of BEFu and BEDh respectively .The inhibition efficiency of additive compounds depends on factors that include the number of adsorption active centers, their charge density, inhibitors molecular size and theirinteraction way with metal surface. In the light of the given data, we may assert that the steel sample weight loss decreases with inhibitor usage and vice-versa. The noticed decrease takes place due to the fact following which obtained Schiff bases prevent the formation of layer on the metal surface. In fact, the inhibition generates thanks to the Schiff bases S-heterocyclic, O-heterocyclic, azomethine group (-CH=N-) and aromatic cycles [35,36].

Table.1. Corrosion parameters obtained from weight loss measurements of mild steel XC48 in 1M HCl containing various concentrations of the Schiff base compounds **BEDh** and **BEFu** at 25 °C

Inhibitor	***C* (mol/l)**	***Δm* (g)**	***W*(mg.cm^{-2}.h^{-1})**	$IE_g(\%)$	θ
	Blank	0.599	0.003119	/	/
BEDh	5x10^{-6}	0.2230	0.001161	62.77	0.6277
	1,0x10^{-5}	0.1013	0.000527	83.10	0.8310
	5x10^{-5}	0.0331	0.000172	94.48	0.9448
	2.5x10^{-4}	0.0257	0.000133	95.73	0.9573
BEFu	5x10^{-6}	0.0227	0.000568	81.78	0.8178
	1,0x10^{-5}	0.0195	0.000488	84.35	0.8435
	5x10^{-5}	0.0099	0.000051	98.34	0.9834
	2.5x10^{-4}	0.0018	0.000043	98.62	0.9862

3.2.2. Potentiodynamic polarization measurements

The Figure.1 displays the potentiodynamic polarization curves related to the XC48 steel in Schiff bases BEDh and BEFu at diverse concentrations. The parameters corrosion such corrosion potential (E_{corr}), anodic Tafel slope (β_a), cathodic Tafel slope (β_c) and suchlike have been get in extrapolating the Tafel slope. The corrosion rate or the density current (i_{corr}), the percentage inhibition efficiency (*Wp(%))* and surface coverage *(θ),* obtained from the mentioned slope, as shown in Table 2. The BEDh or BEFu addition lightly decreases the corrosion rate, which explains the shift of both anodic and cathodic curves to lower current densities. The noticed occurrence is likely due to the adsorption quality rate of inhibitor and that of the metal oxidation [37, 38].In the case of a corrosion potential more than ±85 mV regarding the blank solution corrosion potential, the inhibitor is merely of anodic or cathodic type [39]. In the case at hand, the adding of the inhibitors of BEDh hand BEFu caused the corrosion potential slide to further negative values inferior to 85 mV. The slide thus occurred pointed to an effect of a mixed -type inhibitor with slight cathodic tendency [40, 41]. The experiences led us to draw the conclusion following which the 92.47% BEFu maximum inhibition effectiveness is gained with 2.5.10^{-4}M concentration. As for, BEDh inhibitor, the

86.45% inhibition effectiveness is gained with 2.510^{-4}M inhibitor concentration. In the light of the obtained data, it is to be asserted that the synthesized Schiff base efficiency inhibition occurred because of the O-heterocyclic atoms and the molecules aromatic rings in the presence that can increase the molecules adsorption on the metal surface. The whole polarization in acidic solution results are in quite agreement with those obtained from the weight loss.

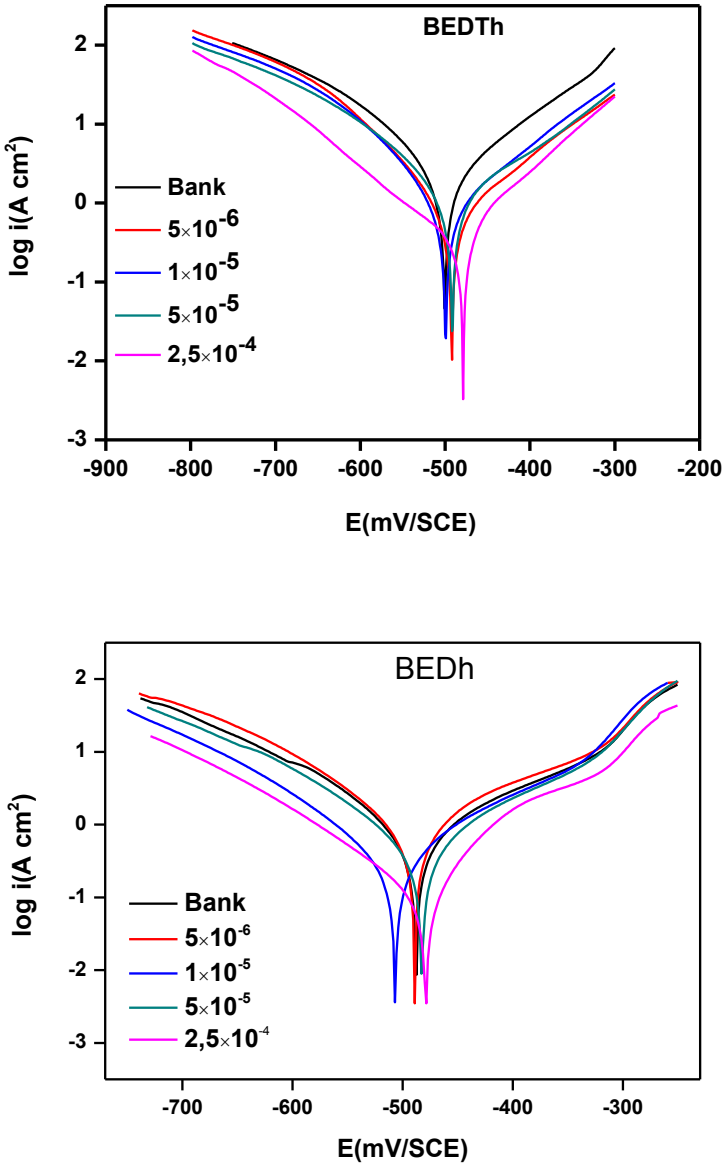

Fig.1. Cathodic and anodic polarization curves obtained at 25°C in 1 M HCl at different concentrations of **BEFu** and **BEDh**

Table. 2. Polarization parameters of mild steel XC48 in 1M HCl solution in the presence and absence of inhibitor **BEDh** and **BEFu** at different concentration at 25°C

Inhibitor	***C*(mol/l)**	E_{corr} **(mV /SCE)**	i_{corr} **(mA/cm^2)**	***Ba*** **(mV /dec)**	***Bc*** **(mV/dec)**	***Wp*(%)**	***θ***
	Blank	-486.4	0.7072	141.9	-104.5	/	/
BEDh	$5x10^{-6}$	-484.7	0.4504	117.4	-103.2	36.31	0.3631
	$1,0x10^{-5}$	-525.2	0.2831	101.6	-96.1	59.96	0.5996
	$5x10^{-5}$	-478.8	0.1274	68.5	-97.6	81.98	0.8198
	$2.5x10^{-4}$	-477.4	0.0958	59.5	-96.3	86.45	0.8645
BEFu	$5x10^{-6}$	-502	0.1074	137	-95	84.81	0.8481
	$1,0x10^{-5}$	-496	0.0995	120	-74	85.95	0.8595
	$5x10^{-5}$	-491	0.0835	118.4	-69	88.19	0.8819
	$2.5x10^{-4}$	-479	0.0532	90.8	-72	92.47	0.9247

3.2.3. Impedance spectroscopy (EIS) measurement

Impedance provides information on the resistive and capacitive behavior at the interface and allows evaluating the performance of the tested compounds as possible inhibitors of metal corrosion. The parameters drawn from Nyquist plots i.e. charge transfer resistance R_{ct}, double layer capacitance C_{dI}, solution resistance R_s and inhibitor efficiency values W_E (%) and surface coverage (θ) are displayed in Table 3.

Table. 3. Electrochemical impedance parameters calculated from Nyquist plots of XC48 in 1M HCl at various concentrations of inhibitor

Inhibitor	***C* (M)**	R_S **(Ω cm^2)**	R_{CT} **(Ω cm^2)**	C_{dl}**(µF cm-^{2})**	W_E**(%)**	**θ**
BEDh	**Blank**	0.588	33.44	2061	/	/
	$5x\ 10^{-6}$	0.977	57.12	1347	41.45	0.414
	10^{-5}	0.851	71.72	1129	53.37	0.531
	$7.5x\ 10^{-5}$	0.6521	101.1	792.4	66.92	0.669
	$2.5x\ 10^{-4}$	1.481	150.5	640.5	77.78	0.777
BEFu	$5x10^{-6}$	0,691	55.68	398,9	39.94	0.399
	10^{-5}	0,552	96.30	351,4	65.06	0.650
	$7.5x\ 10^{-5}$	0,532	118.44	341,3	71.54	0.715
	$2.5x\ 10^{-4}$	0,410	363.18	329,0	90.79	0.907

We note, for all the concentrations used, the presence of a single capacitive loop corresponding to a charge transfer process Figure.2.

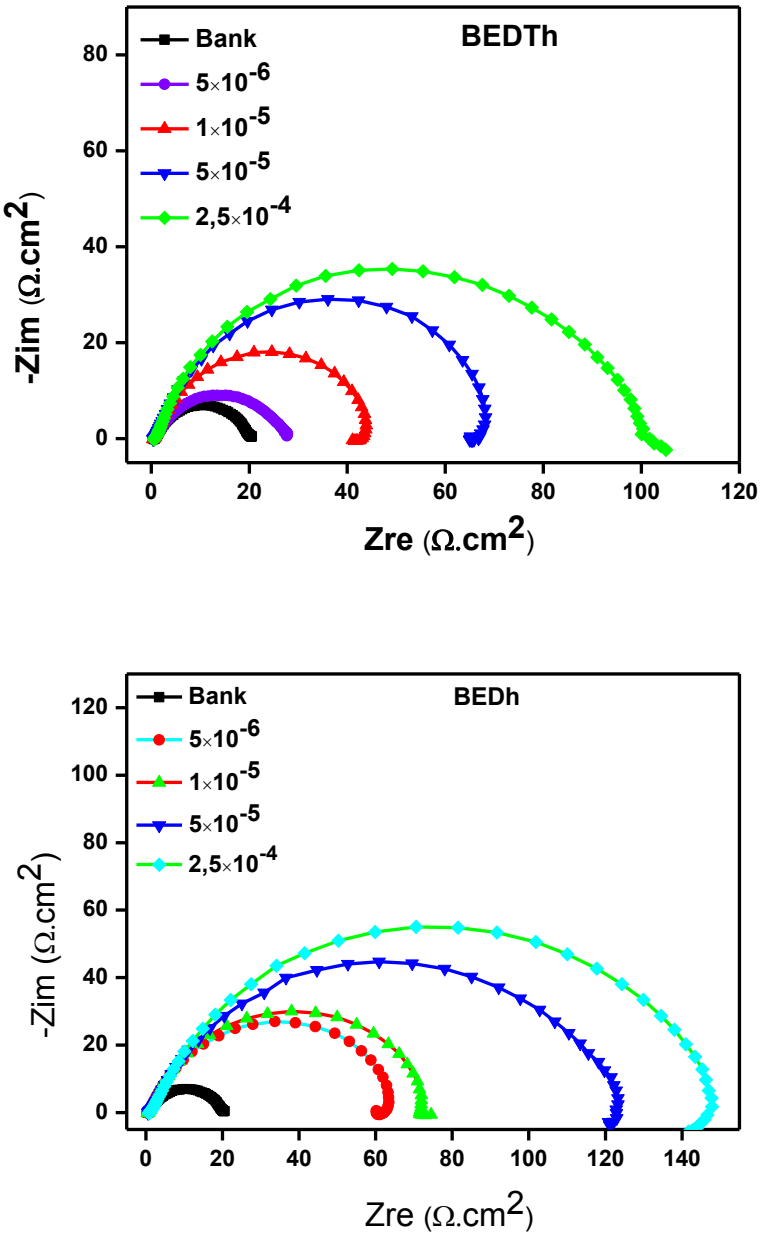

Fig.2. Nyquist plots of XC48 in 1M HCl solutions without and with various concentrations of BEFu and BEDh at 25°C

The results obtained using this technique is represented as diagrams of Nyquist. The diameters of the capacitive semicircles increase with the growth of the inhibitor concentration. It is clear from all the curves that the impedance of the carbon steel in the test solution was significantly modified after addition of BEFu and BEDh inhibitors. The experiences led us to draw the conclusion following which the 90.79 % BEFu maximum inhibition effectiveness is gained with $2.5.10^{-4}$M concentration. As for, BEDh inhibitor, the 77.78% inhibition effectiveness is

gained with 2.510^{-4}M inhibitor concentration. The values of charge transfer resistance, *Rct* increase in the inhibitory system than the uninhibited system. High strength is associated with the slowing of the corrosion system and decreases the active surface required for the corrosion reaction [42], the decrease in the capacity of the C_{dl} double layer with inhibitor concentration is probably due to a decrease in the constant local dielectric and / or an increase in the thickness of a protective layer on the surface of the electrode [43,44]. The inhibition effectiveness obtained with electrochemical impedance spectroscopy is in good agreement with the results obtained by potentiodynamic polarization and weight loss experiments.

We note, for all the concentrations used, the presence of a single capacitive loop corresponding to a charge transfer process Figure.2.

3.2.4. Adsorption isotherm

It should be noted that the inhibition of metal corrosion by organic compounds is explained by their adsorption on the metal surface, the physisorption, the chemical adsorption or mixed adsorption physisorption tending to chemisorption or vice versa. The chemical adsorption process involves a transfer or sharing of electrons between the molecules of the inhibitor and the "d" unsaturated orbital's of the metal surface. In general, adsorption is via the orbitals of organic molecules with weakly bound electrons. The Langmuir isotherm, the equilibrium constant for adsorption–desorption process(K_{ads})and the standard Gibbs free energy of adsorption (ΔG^0_{ads}) can be calculated by equations (7), (8) and (9) [45,46].

$$Cinh/_{\theta} = \frac{1}{K_{ads}} + C_{inh} \qquad (7)$$

$$K_{ads} = \frac{1}{55.5} exp\left(\frac{-\Delta G^{\circ}_{ads}}{RT}\right) \qquad (8)$$

$$\Delta G^{\circ} = -RTln(55{,}5Kads) \qquad (9)$$

Where C_{inh} is the inhibitor concentration, θ is the surface coverage, Kads is the constant for adsorption were calculated from the intercepts of Langmuir adsorption isotherms, is related to the standard free energy of adsorption $\Delta G°_{abs}$ (kj.mol^{-1}) by the equation (20). The 55.5 is the concentration of water in solution expressed in moles per liter, R=8.3144 J K^{-1}mol^{-1} is universal gas constantand T is the temperature in K.

The curve C_{inh} / θ as a function of concentration is linear for BEFu and BEDh at 298k in hydrochloric medium Figure.3, this shows that the adsorption of BEFu and BEDh on the surface of the steel in a hydrochloric medium obeys the adsorption isotherm of Langmuir. The correlation coefficient (R^2) was used to choose the isotherm it is found that the linear correlation coefficients are close to 1(R^2 = 0.99046 for BEFu and R^2 = 0.9998 for BEDh). The values of

the constant K_{ads} and the adsorption energy ΔG^{0}_{ads} calculated from the Langmuir isotherm are collated in Table 4. Before interpreting the nature and character of adsorption, Bransoi and al [47], estimated that for values of $\Delta G°_{ads}$ between 0 and -20 KJ / mol, there is physisorption (physical adsorption). On the other hand, Moretti and al.[48], showed that those close to -40 kJ/ mol^{-1} or higher involve charge transfer between organic molecules and the metal surface (chemisorptions)[49,50].The experiences led us to draw the conclusion following the values of $\Delta G°_{ads}$ which are calculated as -39.33 kJ / mol for BEDh and -38.89 kJ / mol for BEFu. This indicates that the adsorption of the compounds studied on the surface of carbon steel is chemisorptions.

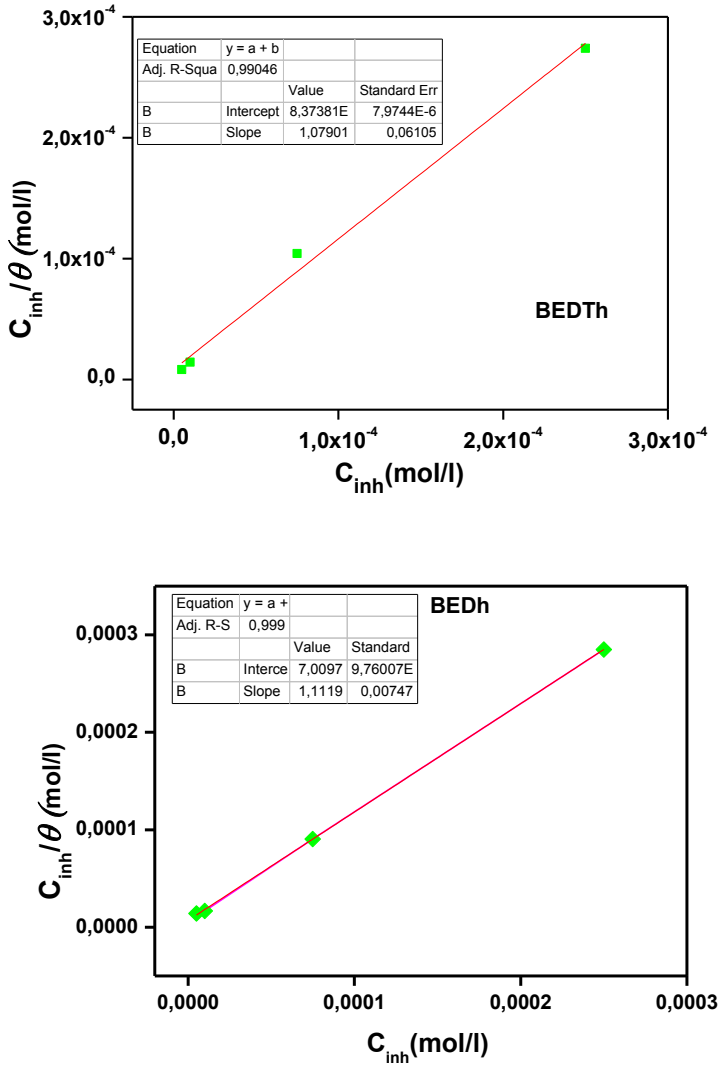

Fig.3. Langmuir adsorption plot for mild steel in the presence of BEFu and BEDh at 25°C

Table .4. Thermodynamic parameters for the adsorption of **BEDh** and **BEFu** on the XC48 in 1 M HCl

	Slope	K_{ads}	R^2	ΔG_{ads}^0 (kJ mol^{-1})
BEDh	1.1119	$1.42659.10^5$	0.9998	-39.33
BEFu	1.07901	$1.19419.10^5$	0.9904	-38.89

3.3 DFT studies

3.3.1. Geometry optimization

The optimized ground state structures for BEDh and BEFu has been illustrated in Figure.4.

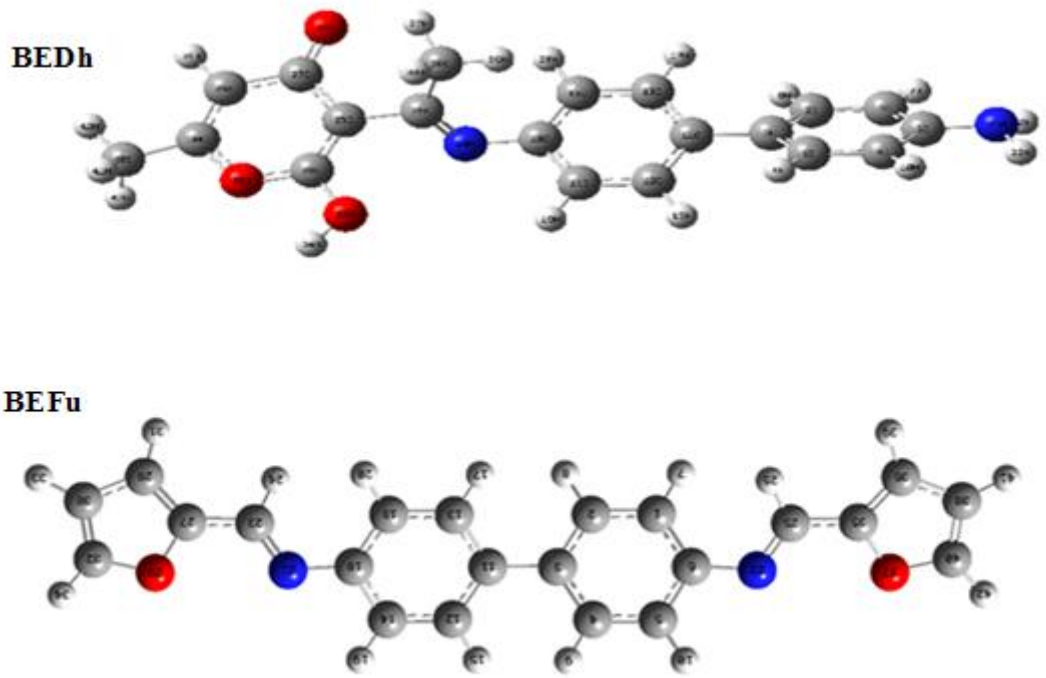

Fig.4. The optimized molecular structure of BEDh and BEFu using DFT (B3LYP)/6-31G(d,p)

The optimized parameters of the two ligands calculated by B3LPY/6-31G (d,p) are listed in Table 5 and 6. All the bond lengths and bond angles in heterocyclic rings are in the common range.The "C–C" and"C–O" bond distances are found to be in the range from1.48 - 1.085A^0, 1.3531-1.554$A^0$and 1.3688A°-1.3556A° , 1.2029-1.4265 A° for BEFu and BEDh, respectively, while for "C=N", these values are 1.2737Å for BEDh and 1.4024Å for BEFu. All the "C-C-C" angles lay between 117.53° to 121.61°. All the dihedral angles in two molecules are between -179°and +179° showing the non-planar structure of BEDh and BEFu. According to Karimi and

al [51], smaller length of bonds means that the molecule has a better stability. In our case, it was observed that the BEFu system is the most stable compound in this study, because has the least amount of length bonds.

Table.5. Selected optimized parameters of **BEDh** by B3LYP/6-31G(d,p) basis set

bond	**Bond lengths (Å)**	**bond**	**Bond angles (θ)**	**bond**	**Dihedral angles (θ)**
C1-C2	1.3881	C2-C1-C6	120.7631	C6-C1-C2-C3	0.059
C1-C6	1.4026	C2-C1-H7	119.7537	C6-C1-C2-H8	178.6574
C1-H7	1.0791	C6-C1-H7	119.4776	H7-C1-C2-C3	-179.0734
C2-C3	1.4031	C1-C2-C3	121.8193	H7-C1-C2-H8	-0.475
C2-H8	1.0844	C1-C2-H8	118.7564	C2-C1-C6-C5	-0.0699
C3-C4	1.4032	C3-C2-H8	119.4096	C2-C1-C6-N21	-177.0693
C3-C11	1.482	C2-C3-C4	116.8949	H7-C1-C6-C5	179.0648
C4-C5	1.388	C2-C3-C11	121.5374	H7-C1-C6-N21	2.0655
C4-H9	1.0842	C4-C3-C11	121.5677	C1-C2-C3-C4	-0.0945
C5-C6	1.4026	C3-C4-C5	121.7925	C1-C2-C3-C11	179.8544
C5-H10	1.0857	C3-C4-H9	119.3952	H8-C2-C3-C4	-178.6839
C6-N21	1.3959	C5-C4-H9	118.7905	H8-C2-C3-C11	1.265
C11-C12	1.4029	C4-C5-C6	120.7948	C2-C3-C4-C5	0.1484
C11-C13	1.4049	C4-C5-H10	119.6985	C2-C3-C4-H9	-178.1314
C12-C14	1.3899	C6-C5-H10	119.5041	C11-C3-C4-C5	-179.8004
C12-H15	1.0844	C1-C6-C5	117.9351	C11-C3-C4-H9	1.9198
C13-C16	1.388	C1-C6-N21	120.9757	C2-C3-C11-C12	-143.7432
C13-H17	1.0844	C5-C6-N21	121.0198	C2-C3-C11-C13	36.9574
C14-C18	1.4014	C3-C11-C12	121.3431	C4-C3-C11-C12	36.2033
C14-H19	1.084	C3-C11-C13	121.3634	C4-C3-C11-C13	-143.0961
C16-C18	1.4009	C12-C11-C13	117.2901	C3-C4-C5-C6	-0.1677
C16-H20	1.0836	C11-C12-C14	121.6105	C3-C4-C5-H10	-179.5777
C18-C25	1.406	C11-C12-H15	119.4782	H9-C4-C5-C6	178.1222
N21-H22	1.0095	C14-C12-H15	118.8961	H9-C4-C5-H10	-1.2878
N21-H23	1.0095	C11-C13-C16	121.5092	C4-C5-C6-C1	0.1231
N24-C25	1.2737	C11-C13-H17	119.3897	C4-C5-C6-N21	177.1211
C25-C26	1.5046	C16-C13-H17	119.056	H10-C5-C6-C1	179.5343
C25-C40	1.5054	C12-C14-C18	120.476	H10-C5-C6-N21	-3.4678
C26-C27	1.4408	C12-C14-H19	120.1833	C1-C6-N21-H22	-158.4989
C26-C28	1.371	C18-C14-H19	119.3316	C1-C6-N21-H23	-26.1389
C27-O34	1.4265	C13-C16-C18	120.6245	C5-C6-N21-H22	24.5946
C27-O35	1.2029	C13-C16-H20	120.7319	C5-C6-N21-H23	156.9546
C28-C29	1.431	C18-C16-H20	118.6421	C3-C11-C12-C14	179.7369
C28-O32	1.3489	C14-C18-C16	118.4576	C3-C11-C12-H15	1.1721
C29-C30	1.3531	C14-C18-N24	122.184	C13-C11-C12-C14	-0.9362
C29-H31	1.0826	C16-C18-N24	119.1363	C13-C11-C12-H15	-179.5011
C30-O34	1.3425	C6-N21-H22	115.107	C3-C11-C13-C16	179.4968
C30-C36	1.492	C6-N21-H23	115.1542	C3-C11-C13-H17	1.9607

O32-H33	0.9631	H22-N21-H23	111.8335	C12-C11-C13-C16	0.1701

Table.6. Selected optimized parameters of **BEFu** by B3LYP/6-31G(d,p) basis set

bond	**Bond lengths (Å)**	**Bond**	**Bond angles (θ)**	**bond**	**Dihedral angles (θ)**
C1-C2	1.3905	C2-C1-C6	120.5836	C6-C1-C2-C3	0.1811
C1-C6	1.4072	C2-C1-H7	119.6227	C6-C1-C2-H8	-177.5105
C1-H7	1.0859	C6-C1-H7	119.7253	H7-C1-C2-C3	177.1652
C2-C3	1.4062	C1-C2-C3	121.4551	H7-C1-C2-H8	-0.5264
C2-H8	1.086	C1-C2-H8	119.1462	C2-C1-C6-C5	1.5428
C3-C4	1.4074	C3-C2-H8	119.3589	C2-C1-C6-N22	178.9615
C3-C11	1.4815	C2-C3-C4	117.5398	H7-C1-C6-C5	-175.4382
C4-C5	1.3886	C2-C3-C11	121.1003	H7-C1-C6-N22	1.9805
C4-H9	1.0857	C4-C3-C11	121.3542	C1-C2-C3-C4	-0.9818
C5-C6	1.4052	C3-C4-C5	121.3239	C1-C2-C3-C11	179.8792
C5-H10	1.0852	C3-C4-H9	119.4389	H8-C2-C3-C4	176.705
C6-N22	1.4024	C5-C4-H9	119.2293	H8-C2-C3-C11	-2.4341
C11-C12	1.4074	C4-C5-C6	120.8098	C2-C3-C4-C5	0.0382
C11-C13	1.4062	C4-C5-H10	120.9191	C2-C3-C4-H9	179.0085
C12-C14	1.3886	C6-C5-H10	118.2534	C11-C3-C4-C5	179.175
C12-C15	1.0857	C1-C6-C5	118.2447	C11-C3-C4-C9	-1.8547
C13-C16	1.3905	C1-C6-N22	124.0374	C2-C3-C11-C12	144.3177
C13, H17	1.086	C5-C6-N22	117.67	C2-C3-C11-C13	-36.5762
C14-C18	1.4052	C3-C11-C12	121.3542	C4-C3-C11-C12	-34.7883
C14-H19	1.0852	C3-C11-C13	121.1003	C4-C3-C11-C13	144.3177
C16-C18	1.4072	C12-C11-C13	117.5398	C3-C4-C5-C6	1.7175
C16, H20	1.0859	C11-C12-C14	121.3239	C3-C4-C5-H10	-179.8395
C18, N21	1.4024	C11-C12-H15	119.4389	H9-C4-C5-C6	-177.255
N21-C23	1.284	C14-C12-H15	119.2293	H9-C4-C5-H10	1.1881
N22, C25	1.284	C11-C13-C16	121.4551	C4-C5-C6-C1	-2.4806
C23-H24	1.0993	C11-C13-H17	119.3589	C4-C5-C6-N22	179.9345
C23, C27	1.4419	C16-C13-H17	119.1462	H10-C5-C6-C1	179.0357
C25-H26	1.0993	C12-C14-C18	120.8096	H10-C5-C6-N22	1.4509
C25-C35	1.4419	C12-C14-H19	120.919	C1-C6-N22-C25	35.6726
C27-C28	1.3757	C18-C14-H19	118.2536	C5-C6-N22-C25	-146.895
C27-O29	1.3688	C13-C16-C18	120.5836	C3-C11-C12-C14	179.1749
C28-C30	1.4247	C 13-C16-H20	119.6229	C3-C11-C12-H15	-1.8547
C28-H31	1.0808	C18-C16-H20	119.7251	C13-C11-C12-C14	0.0382
O29-C32	1.3556	C14-C18-C16	118.2449	C13-C11-C12-H15	179.0086
C30-C32	1.3657	C14-C18-N21	117.6703	C3-C11-C13-C16	179.8791
C30-H33	1.0801	C16-C18-N21	124.0368	C3-C11-C13-H17	-2.4341
C32-H34	1.0792	C18-N 21-C23	119.7448	C12-C11-C13-C16	-0.9819
C35-C36	1.3757	C6-N22-C25	119.7456	C12-C11-C13-H17	176.705
C35-O37	1.3688	N21-C23-H24	122.899	C11-C12-C14-C18	1.7176
C36-C38	1.4247	N21-C23-C27	123.1612	C11-C12-C14-H19	-179.8393
C36-H39	1.0808	H24-C23-C27	113.9327	H15-C12-C14-C18	-177.255

O37-C40	1.3556	N22-C25-H26	122.8992	H15-C12-C 14-H19	1.1881
C38-C40	1.3657	N22-C25-C35	123.1611	C11-C13-C16-C18	0.1813
C38-H41	1.0801	H26-C25-C35	113.9327	C11-C13-C16-H20	177.1652

3.3.2. Mulliken atomic charges

To perform any calculation in a quantum chemical application, Mullikan atomic charges values in molecular systems are crucial. That is, atomic charges affect dipole moments, molecular polarization abilities, electronic structure, and many other properties of molecular systems [52]. The electronic charges on the different ligands atoms suggest the presence of donor and acceptor pairs involving a charge transfer in the molecule. The charges in question values allowed us to assess the processes of electro-negativity equalization and the charge transfer in chemical reactions [53,54]. The Mulliken atomic charges for BEDh and BEFu compounds calculated by the B3LYP/6-31 G(d,p) level in gas-phase are presented in Table 7. The Mulliken charge distribution shows that the azomethine nitrogen atom N is more negative (~ -0.496) as compared to the other "N21","N24"= -0.466 for BEDh and -0.4747 for BEFu. The charge on azomethine"C23", "C25" atoms 0.1877,0.1979 for BEDh and 0.8813, 0.08814 for BEFu may be due to the charge delocalization. It has also been observed that some "C" atoms are positive and some are negative.

Table .7. Mulliken atomic chargescalculated by B3LYP/6-31G(d, p) of **BEDh** and **BEFu**

BEDh				**BEFu**			
Atom	charge	Atom	charge	Atom	charge	Atom	charge
C1	-0.084374	C23	0.187770	C1	-0.105960	C23	0.088139
C2	-0.062612	N24	-0.466454	C2	-0.131564	H24	0.089193
C3	-0.066566	C25	0.169718	C3	0.069667	C25	0.088140
C4	-0.063019	C26	-0.265603	C4	-0.124748	H26	0.089192
C5	-0.045711	C27	0.380460	C5	-0.099132	C27	0.311494
C6	0.048639	C28	0.371054	C6	0.248672	C28	-0.136646
H7	0.080672	C29	-0.201504	H7	0.083843	O29	-0.429854
H8	0.085033	C30	0.168806	H8	0.086012	C30	-0.137980
H9	0.086450	H31	0.108125	H9	0.089071	H31	0.104974
H10	0.093208	O32	-0.377212	H10	0.095734	C32	0.150270
C11	-0.087023	H33	0.259116	C11	0.069666	H33	0.103730
C12	-0.055808	O34	-0.163469	C12	-0.124748	H34	0.119852
C13	-0.066103	O35	-0.473747	C13	-0.131565	C35	0.311495
C14	-0.103130	C36	-0.271916	C14	-0.099133	C36	-0.136646
H15	0.082482	H37	0.154666	H15	0.089071	O37	-0.429853
C16	-0.073720	H38	0.144499	C16	-0.105961	C38	-0.137980
H17	0.084709	H39	0.149589	H17	0.086012	H39	0.104974
C18	0.219702	C40	-0.201243	C18	0.248673	C40	0.150270

H19	0.083342	H41	0.126226	H19	0.095735	H41	0.103730
H20	0.091871	H42	0.132048	H20	0.083843	H42	0.119852
N21	-0.496599	H43	0.105745	N21	-0.474767		
H22	0.211883			N22	-0.474767		

3.3.3. Frontier Molecular Orbital Analysis

Molecular orbital's (HOMO-LUMO) and their properties such as energy are very useful for physicist and chemists and are very important parameters for quantum chemistry. Both the highest occupied molecular orbital (HOMO) and lowest unoccupied molecular orbital (LUMO) are the main orbital's which take part in chemical stability. E_{HOMO} is generally associated with the electron donating ability of a molecule. High values of E_{HOMO} are likely to denote the tendency of the molecule to donate electrons to acceptor molecules of lower energy MO. E_{LUMO}, indicates the ability of the molecule to accept electrons [55]. The binding ability of the molecule increases with increasing HOMO and decreasing LUMO energy values. Thus, the lower the value of E_{LUMO}, the most probable it is that the molecule would accept electrons.

The HOMO and LUMO energy calculated by B3LYP/6-31G(d,p) method for both molecules is shown below. This electronic absorption corresponds to the transition from the ground to the first excited state and is mainly described by one electron excitation from the highest occupied molecular orbital to the lowest unoccupied molecular orbital. While the energy of the HOMO describes the ionization potential, LUMO energy is concerned by the electron affinity Energy.

The 3D plots of the frontier orbital are HOMO and LUMO, for the both molecules are as shown in Figure 5. The green and red solid regions in Figure.5 represent the MOs with completely opposite phases. The positive phase of the molecule is represented in red color and negative phase in green color. It can be seen that, the HOMO for the molecules BEDh and BEFu is delocalized almost over the whole p-conjugated system, While the LUMO, and is also delocalized over the whole molecules.

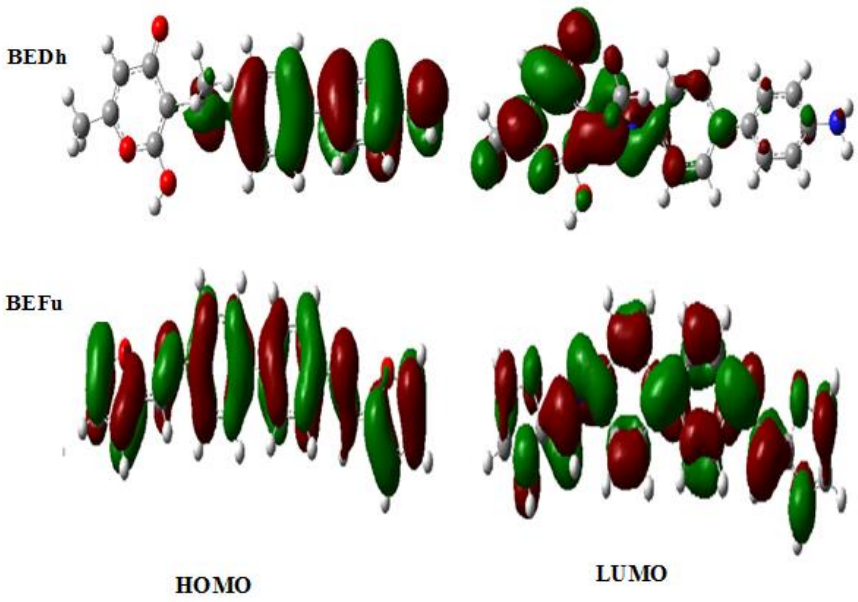

Fig.5. HOMO and LUMO electron density distributions of neutral forms of BEDh and BEFu.

The energy gap (ΔE) represents the chemical reactivity of compounds. A molecule with a small energy gap is more polarizable and is generally associated with a high chemical reactivity, low kinetic stability and also termed as soft molecule [56].In present study, values of ΔE followed the order: BEDh (3.5809eV) > BEFu (3.5613eV). As depicted in Table 8, compound BEDh has a largest energy gap than BEFu. So BEFu is more reactive and less stable than BEDh.

3.3.4. Global reactivity descriptors

Energies of *HOMO* and *LUMO* played a major role in electron transfers in molecules. By using E_{HOMO} and E_{LUMO} values for a molecule, the global chemical reactivitydescriptors of molecules such as hardness *(η)*, chemical potential *(μ)*, softness *(S)*, electronegativity *(χ)* and electrophilicityindex*(ω)* can be measured by using Koopman's theorem for closed-shell molecules.A molecule having high ionization potential *(I)* or electron affinity *(A)* loses or admits electron hardly [57,58]. By Koopmans' approximation [59], the ionization potential and electron affinity of any molecule can be calculated using the relations.

$$I = -E_{HOMO} \qquad (10)$$

$$A = -E_{LUMO} \qquad (11)$$

Koopmans` theorem for closed-shell molecules [60] results in the hardness of the molecule.

$$\eta = (I - A)/2 \qquad (12)$$

The chemical potential of the molecule:

$$\mu = -\frac{I + A}{2} \qquad (13)$$

The softness of the molecule*:*

$S = 1/\eta$ (14)

The electro negativity of the molecule:

$\chi = \frac{I + A}{2}$ (15)

The electrophilicity index of the molecule:

$\omega = S.\mu^2$ (16)

The energy obtained at the end of a geometry optimization is the total potential energy of the molecule. The potential energy is the sum of 4 terms:(1) the kinetic energies of the electrons; (2) the electrostatic attraction between the electrons and the nuclei (a very, very negative quantity); (3) the electrostatic repulsion between the electrons (a very positive quantity); and (4) the electrostatic repulsion between the atomic nuclei at the geometry of the molecule (a very positive quantity). The calculated total energy for both molecules is given in Table 8. The total energy of (-1108.4226 au) obtained for BEDh is lower than the one obtained for BEFu(-1107.8875au). This indicates that The BEDh is more stable and less reactive. Ionization energy is an important descriptor of the chemical reactivity of atoms and molecules. High ionization energy designates high stability and chemical inertness and small ionization energy specifies high reactivity of the atoms and molecules [61]. The low ionization energy "*IE*= 5.1929eV" of BEDh indicates the high reactivity of this molecule.

Table.8. Comparison of *HOMO*, *LUMO*, energy gaps (*HOMO–LUMO*) and related molecular properties of **BEDh** and **BEFu**

MolecularEnergy	**BEDh**	**BEFu**
E_{TOT}***(au)***	-1108.4226	-1107.8875
E_{LUMO} **(eV)**	-1.6119	-1.7420
E_{HOMO} **(eV)**	-5.1929	-5.3034
Energy gap (ΔE)(eV)	3. 5809	3.5613
Ionization Potential (*I)* (eV)	5.1929	5.3034
Electron affinity *(A*) (eV)	1.6119	1.7420
Chemicalpotential (μ) (eV)	-3.4024	-3.5227
Global Hardness (η) (eV)	1.7904	1.7806
Global Softness (S) (eV)	206.7704	207.9080
Electronegativity (χ) (eV)	3.4024	3.5227
Electrophilicity (ω) (eV)	3.2328	3.4845

Electronegativity measures the capacity of an atom to attract electrons to it. The target molecules have electronegativity of (3.4024eV) for BEDh and (3.5227eV) for BEFu. So BEFu has low capacity of attracting electrons from the neighboring molecules than the BEDh. Hardness (η) is essential properties to measure the stability and reactivity of molecules. A hard molecule has a great energy gap and a soft molecule has a small energy gap [62]. In our present study BEFu with low hardness value (1.7806 eV) compared with other compound have a low energy gap. Normally, the molecule with the least value of global hardness (hence the highest value of global softness) is expected to have the highest reactivity [63]. Parr and al, introduced the concept of Electrophilicity *(ω)* as a global reactivity index similar to the chemical hardness and chemical potential [64], is a descriptor of reactivity that allows a quantitative classification of the global electrophilic comportment of a molecule within a relative scale. Parr and al. have proposed the Electrophilicityas a measure of energy lowering owing to maximal electron flow between acceptor and donor. The electrophilicity index *(ω)* has been used as structural depictor for the analysis of the chemical reactivity of molecules [65]. Electrophilicity measures the propensity of a species to accept electrons.

A good, more reactive, nucleophile is characterized by a lower value of *(ω),* in opposite a good electrophile is characterized by a high value of (ω). The BEFu with (ω=3.4845eV) is a good electrophile. BEDh has lower value, so it isgood, more reactive and nucleophile.Physically, electronic chemical potential (μ) describes the escaping tendency of electrons from an equilibrium system. The electronic chemical potential is defined as the negative of electro negativity of a molecule [66].The values of μ were calculated and presented in Table 8. The greater the electronic chemical potential, the less stable or more reactive is the compound. From the Table 8, the BEDh (-3.5227 eV) is less stable and more reactive in the gas phase and BEFu (-3.4024 eV) is more stable and less reactive.

3.3.5. Molecular Electrostatic Potential (MEP)

In order to grasp the molecular interactions, the molecular electrostatic potential (MEP) is used. The molecular electrostatic potential is the potential that a unit positive charge would experience at any point surrounding the molecule due to the electron density distribution in the molecule [67, 68].The 3D plot of molecular electrostatic potential (MEP) for BEDh and BEFu are shown in Figure.6.

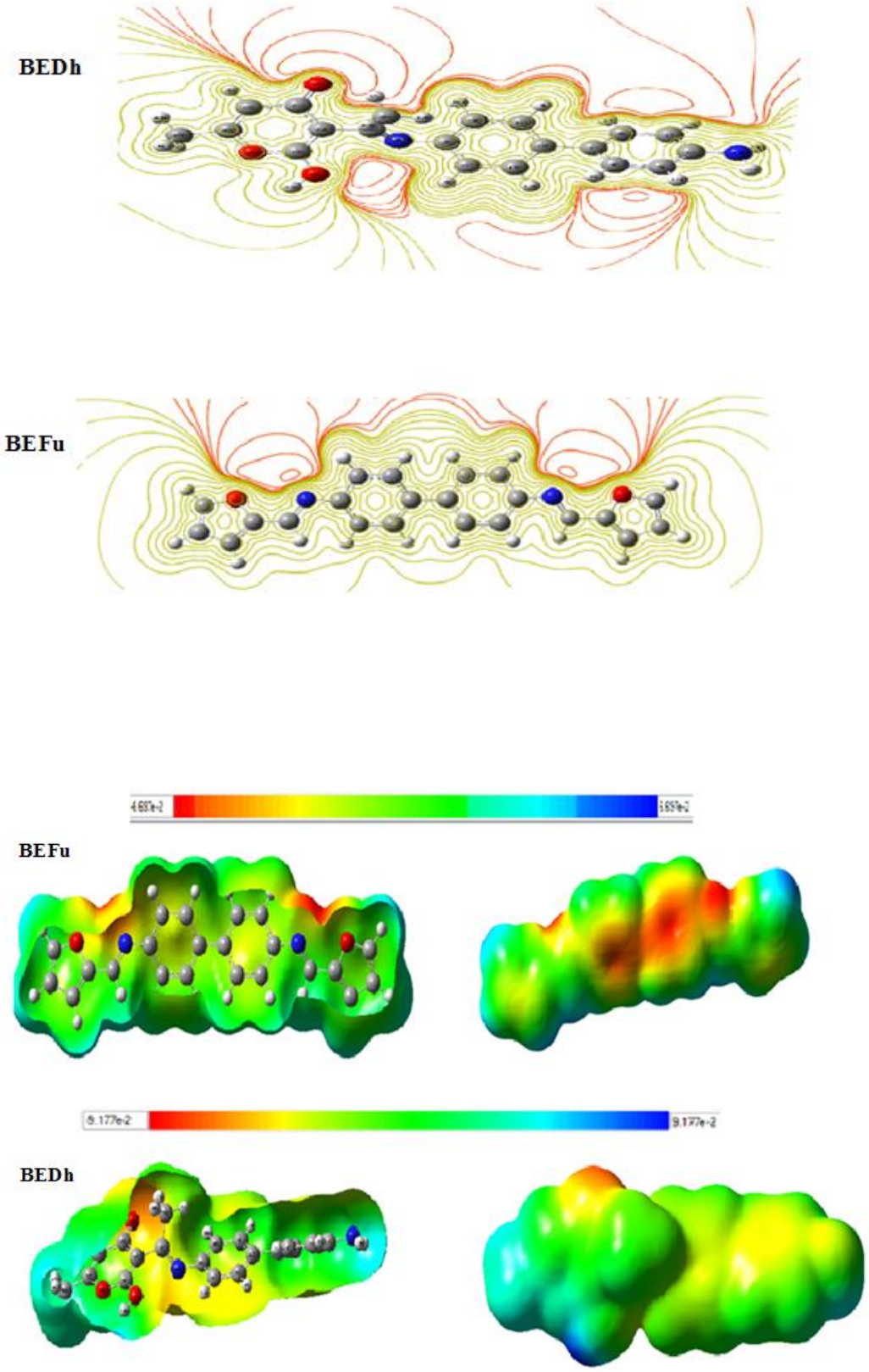

Fig.6. Contour map of electrostatic potential and total electron density surface mapped with electrostatic potential

This is based on the electron density at different points on the molecule. The red color in the map indicates the negatively charged portion and the blue color indicates the positive region, while the green color indicates the neutral region. The potential values in this molecule ranges from (-8.105 a.u) deepest red to (+8.105 a.u) deepest blue for BEDh and from (-1.107a.u) deepest red to (+1.107a.u) deepest blue for BEFu. As can be seen from the map, the regions surrounding the sulfur and oxygen atoms are strongly negative, while the H atoms in the ring and amine groups are positive; among them the Hydrogen atoms in the amino function are more positive than them in ring groups.

4. CONCLUSION

Two new heterocyclic Schiff's base BEDh and BEFu were synthesized and their molecular structures were established using UV–Visible, FT-IR and ^{1}H-NMR spectroscopies. The inhibition efficiency of these compounds on corrosion of mild steel in 1 M HCl was investigated and compared to their quantum chemical calculations. The potentiodynamic polarization curves results indicate that the studied compounds acts as a mixed-type inhibitor in 1 M HCl, their inhibition efficiencies increase with inhibitors concentration in the order: BEFu > BEDh with a maximum value of 92.47 % at $2{,}5\text{x}10^{-4}$ M. The adsorption of the inhibitor molecules obeys Langmuir adsorption isotherm, the negative sign of the adsorption free energy $(\Delta G°)$ involves both physisorption and chemisorption. The molecular properties quantum such as Ionization Potential (I), Electron affinity (A), Global Hardness (η), Chemical potential (μ) and Global Electrophilicity (ω) were calculated by DFT method and discussed. The theoretical calculations are in good agreement with the experimental results; they show that both O-heterocyclic derivatives have interesting molecular structures for inhibiting the corrosive process.

5. REFERENCES

[1] M. Akbar Ali, S. E. Livingstone, and D. J. Phillips, Metal Chelates of Dithiocarbazic Acid and Its Derivatives, VI. Antiferromagnetic and Ferromagnetic Interactions in Some Copper(H) Complexes of Salicylaldehyde and Acetylacetone Schiff Bases Derived from S-Methyldithiocarbazate. *Inorganica Chimica Acta, 1973, 7.*

[2] H. Schiff, Ann. Der Chem. Und Pharm.1864, 131, 118-119.

[3] Hui Wang, Abul Monsur Showkot Hossain, Qiong Zhang, Jieying Wu, Yupeng Tian, Synthesis, crystal structures and third-order nonlinear optical properties of 4-formylpyridine Schiff base of thiosemicarbazide, and its dinuclear copper(I) and silver(I) complexes. Inorganica Chimica Acta.2014, 414,153–159.

[4] B. Pedras, L. Fernandes, E. Oliveira, L. Rodríguez, M. Manuela M. Raposo, J. L. Capelo, C. Lodeiro, Inorg. Chem. Commun.2009, 12,79-85

[5] L. Mishra, S. K. Dubey, Spectrochim. Acta, Part A.2007, 68,364-368

[6] K. Bhat, K.J. Chang, M.D. Aggarwal, W.S. Wang, B.G. Penn, D.O. Frazier, Mater. Chem. Phys, 1996,44,261-266

[7] I. Finar, vol 2. Organic Chemistry, 5thed, Longman, London, (1973).

[8] A. Gullvich, E. Balenkova, V. Nenajdnko, J. Org. Chem.2005,72,7878-7885

[9] G. Ceyhan, M. Tümer, M. Köse, V. McKee, S. Akar, J. Lumin.2012, 132, 2917-2928

[10] H. Hamani, T. Douadi, M. Al-Noaimi, S. Issaadi, D. Daoud, S. Chafaa, Electrochemical and quantum chemical studies of some azomethine compounds as corrosion inhibitors for mild steel in 1 M hydrochloric acid, Corros, Sci.2014,88, 234-245

[11] D. Daoud, T. Douadi, S. Issaadi, S. Chafaa, Adsorption and corrosion inhibition of new synthesized thiophene Schiff base on mild steel X52 in HCl and H2SO4 solutions, Corros, Sci.2014, 79, 50-58

[12] D. Daoud, T. Douadi, H. Hamani, S. Chafaa, M. Al-Noaimi, Corrosion inhibition of mild steel by two new S-heterocyclic compounds in 1 M HCl: Experimental and computational study, Corros, Sci.2015, 94, 21-37

[13] S. Issaadi, T. Douadi, A. Zouaoui, S. Chafaa, M.A. Khan, G. Bouet, Novel thiophene symmetrical Schiff base compounds as corrosion inhibitor for mild steel in acidic media, Corros, Sci.2011,53, 1484-1488

[14] S. Issaadi, T. Douadi, S. Chafaa, Adsorption and inhibitive properties of a new heterocyclic furan Schiff base on corrosion of copper in HCl 1 M: experimental and theoretical investigation, Appl. Surf, Sci.2014,316, 582–589

[15] A.M. Al-Sabagh, N.M. Nasser, A.A. Farag, M.A. Migahed, A.M.F. Eissa, T. Mahmoud, Structure effect of some amine derivatives on corrosion inhibition efficiency for carbon steel in acidic media using electrochemical and quantum theory methods, Egypt. J. Pet.2013,22, 101-116

[16] S.M. Abd El Haleem, S. Abd El Wanees, E.E. Abd El Aal, A. Farouk, Factors affecting the corrosion behaviour of aluminium in acid solutions. I. Nitrogen and/or sulphur-containing organic compounds as corrosion inhibitors for Al in HCl solutions, Corros, Sci.2013, 68, 1-13.

[17] A. Doner, E.A, Şahin, G. Kardaş, O. Serindağ, Investigation of corrosion inhibition effect of 3-[(2- hydroxy-benzylidene)-amino]-2-thioxo-thiazolidin-4-one on corrosion of mild steel in the acidic medium, Corros, Sci.2013, 66, 278-284

[18] S. Issaadi, T. Douadi, A. Zouaoui, S. Chafaa, M.A. Khan, G. Bouet, Novel thiophene symmetrical Schiff base compounds as corrosion inhibitor for mild steel in acidic media, Corros, Sci.2011, 53, 1484-1488

[19] R. Solmaz, E. Altunbaş, G. Kardaş, Adsorption and corrosion inhibition effect of 2-((5-mercapto-1,3, 4- thiadiazol-2-ylimino)methyl)phenol Schiff base on mild steel; Mater. Chem. Phys. 2011,125, 796-801

[20] ASTM, G 31-72, American Society for Testing and Materials, Philadelphia, PA, 1990.

[21] N. Chafai, S. Chafaa, K. Benbouguerra, D. Daoud, A. Hellal, M. Mehri: Journal of the Taiwan Institute of Chemical Engineers.2017,70, 331-344

[22] Nor Zakiah Nor Hashima, El Hassane Anouarb, Karimah Kassim, Hamizah Mohd Zakic,
Abdulrahman I. Alharthib, ZaidiEmbonge,XPS and DFT investigations of corrosion inhibition of substituted benzylidene Schiff bases on mild steel in hydrochloric acid, Applied Surface Science.2019,476 861–877

[23] ASTM, G 31–72, American Society for Testing and Materials, Philadelphia, PA, 1990

[24] E.E. Abd El Aal, S. Abd El Wanees, A. Farouk, S.M. Abd El Haleem, Factors affecting the corrosion behaviour of aluminium in acid solutions. II. Inorganic additives as corrosion inhibitors for Al in HCl solutions, Corros, Sci.2013, 68, 14–24

[25] M.A. Hegazya, M. Abdallah, M.K. Awad, M. Rezk, Three novel di-quaternary ammonium salts as corrosion inhibitors for API X65 steel pipeline in acidic solution. Part I: Experimental results, Corros, Sci.2014,81 (54-64.

[26] R. Solmaz, Investigation of adsorption and corrosion inhibition of mild steel in hydrochloric acid solution by 5-(4 Dimethylaminobenzylidene)rhodanine, Corros, Sci.2014, 79, 169-17

[27] I. Ahmad, M.A. Quraishi, Corros, Sci.2009,51, 2006-2013

[28] F. Bentiss, M. Lebrini, M. Lagrenee, Corros, Sci.2005,4,2915-2931

[29] M.J. Frisch, G. W. Trucks, H.B. Schlegel, G.E. Scuseria, J.R. Cheeseman, Gaussian 09, Revision, Gaussian, Inc., Wallingford CT, 2009.

[30] C.T. Lee, W. Yang & R. G. Parr, Phys. Rev.1988,37B, 785

[31] R.G. Parr, W.Yang, Density Functional Theory of Atoms and Molecules, Oxford University Press, New York,1989

[32] A. D. Becke, Density-functional thermochemistry. III. The role of exact exchange, Chem. Phys.1993, 98, 5648

[33] G.A. Petersson, M.A. Al-Laham, J. Chem. Phys.1991,94, 6081

[34] ASTM, G 31–72, American Society for Testing and Materials, Philadelphia, PA, 1990

[35] M. Belayachi, H. Serrar, H. Zarrok, A. El Assyry, A. Zarrouk, H. Oudda, S. Boukhris, B. Hammouti, E. E. Ebenso, A. Geunbour, Int. J. Electrochem. Sci.2015,10, 3010

[36] O. L. Riggs, Corrosion inhibitors, C. C. Nathan, NACE, Houston, TX, 2nd ed. 7(1973).

[37] M. Mohammad, R.T. Ali, H. Krister, J. Surf. Deterg.2011,14, 605

[38] E. P. Manuel, O. Crescencio, V. L. Natalya, J. Boanerge, J. Surf. Deterg.2011,14, 211

[39] E. E. Ebenso, U. J. Ekpe, B. I. Ita, O. E. Offiong, U. J. Ibok, Mater. Chem. Phys.1999,60, 79

[40] E.E. Oguzie, Y. Li, F.H. Wang, J. Colloid Interface Sci.2007,310, 90

[41] P.C. Okafor, Y. Zheng, Corros. Sci.2009,51,850

[42] Zerrouki H, Alaoui AF, Belfar ML and Sekhri L. An electrochemical study for corrosioninhibition of iron by a derivative of organic phosphoniumhalid in acid media. J. Fundam.Appl. Sci., 2019, 10(3), 1367-1391

[43] I.B. Obot, N.O. Obi-Egbedi, Corros. Sci. 2010, 52, 198

[44] M. Srivastava, P. Tiwari, S.K. Srivastava, R. Prakash, G. Ji, Electrochemical investigation of Irbesartan drug molecules as an inhibitor of mild steel corrosion in 1 M HCl and 0.5 M H2SO4 solutions, J. Mol. Liq.2017,236, 184-197

[45] Bransoi V, Baibarac M, Brancoi F; International. Cong. Chemical Engineering, Romania.2001, 215.

[46] S. Yesudass, L.O. Olasunkanmi, I. Bahadur, M.M. Kabanda, I.B. Obot, E.E. Ebenso, Experimental and theoretical studies on some selected ionic liquids with different cations/anions as corrosion inhibitors for mild steel in acidic medium, J. Taiwan Inst. Chem. Eng. 2016, 64, 252-268

[47] Moretti G, Guidi F, Grion G; Corros. Sci,2004 ,46, 387

[48] M. Srivastava, P. Tiwari, S.K. Srivastava, A. Kumar, G. Ji. R. Prakash, Low-cost aqueous extract of Pisumsativum peels for inhibition of mild steel corrosion, J. Mol. Liq.2018,254, 357-368

[49] M. Srivastava, P. Tiwari, S.K. Srivastava, R. Prakash, G. Ji, Electrochemical investigation of Irbesartan drug molecules as an inhibitor of mild steel corrosion in 1 M HCl and 0.5 M H2SO4 solutions, J. Mol. Liq. 2017, 236, 184-197.

[50] M.N. El-Haddad, Chitosan as a green inhibitor for copper corrosion in acidic medium, International Int. J. Biol. Macromol. 2013, 55, 142-149.

[51] K. Jug, Z.B. Maksic, in: Theoretical Model of Chemical Bonding, Ed. Z.B. Maksic, Part 3, Springer and Berlin. 1991, 29, 233

[52] S. Fliszar, Charge Distributions and Chemical Effects, Springer, New York, (1983).

[53] I. Ahamad, R. Prasad, M.A. Quraishi, Chem. Phys; 2010.

[54] E.E. Ebenso, Arslan, T. Kandemirli, Theoretical studies of some sulphonamides as corrosion inhibitors for mild steel in acidic medium, International Journal of Quantum Chemistry.2010, 110, 14, 2614-2636,

[55] K. Govindarasu, E. KavithaSpectrochimica Acta Part A. 2014, 133,799-810.

[56] D.M. Burland, R.D. Miller, C.A.Walsh, Chem. Rev. 1994, 94, 31-75

[57] V.M. Geskin, C. Lambert, J.L. Brédas, J. Am. Chem. Soc. 2003,125,15651-15658

[58] D.A. Kleinman, Phys. Rev. 1977, 126, 1962-1979

[59] SandipK.R., Nazmul I., DulalC.G., J. Quant. Infor. Sci. 2011, 1 87-95.

[60] R. Hasanov, M. Sadikglu, S. Bilgic, Appl. Surf. Sci. 2007, 253, 3913

[61] E. E. Ebenso, D.A. Isabirye, N.O.Eddy, Int. J. Mol. Sci. 2010, 11, 2473-2498.

[62] R. G. Parr, L. V. Szentpaly, S. J. Liu, Am. Chem. Soc. 1999, 121, 1922.

[63] P. K. Chattaraj, U. Sarkar, D. R. Roy, Chem. Rev. 2006,106, 2065.

[64] N. Surendra Babu D. Jayaprakash, Journal of Chemical and Pharmaceutical Research. 2015, 7(4),1155-1160

[65] E. Al Shamaileh. Computational Chemistry. 2014, 02, 43-49

[66] M. Bouklah, H. Harek, R. Touzani, B. Hammouti, Y. Harek, Arab. J. Chem. 2010, 08,008

[67] K. Gokula Krishnan, R. Sivakumar, V. Thanikachalam, H. Saleem, M. Arockia doss, Spectrochim. Acta Part A., 144, 29-42(2015).

[68] B. S. Kusmariya, A.P. Mishra, J. Mol. Struct. 2015, 1101,176

How to cite this article:
Madani A, Sibous L**,** Bentouhami E. Synthesis, characterization, corrosion inhibition of mild steel by two schiff bases in hcl and density functional theory studies. J. Fundam. Appl. Sci., 2021, 13*(2), 864-891*.